

Ice processes and organic matter in space: observations and laboratory simulations

G. M. Muñoz Caro¹ and R. Martín-Doménech¹

¹ Centro de Astrobiología (CAB), INTA-CSIC, Torrejón de Ardoz, Madrid, Spain, munozcg@cab.inta-csic.es

Abstract

The formation of ice mantles on interstellar and circumstellar dust grains is governed by the accretion and desorption processes. Thermal processing of astrophysical ices takes place in circumstellar environments, near protostars, or already formed stars (comets and other icy bodies). Temperature-programmed desorption experiments of ice composed of various molecular components (H₂O, CO, CO₂, CH₃OH, and NH₃) were dedicated to reproduce the heating of circumstellar ices in hot cores, and serve to interpret the measurements of volatiles that mass spectrometers on board the ESA-Rosetta cometary mission are performing on comet 67P/Churyumov-Gerasimenko. But the presence of gas-phase molecules in the coldest regions, such as dark interstellar clouds, remains unexplained. UV-photodesorption is a plausible non-thermal desorption process. The UV-absorption cross-section and the photo-desorption rate of these species were measured to estimate the effect of photo-processing of ice in interstellar clouds and the solar nebula.

Certain species detected in the gas were probably formed in dust grains. The synthesis of UV, X-ray and ion irradiation products in pre-cometary ice was studied experimentally. The organic matter of prebiotic interest formed by irradiation and heating of ice mantles might be preserved to some degree in Halley-like comets and some asteroids. Indeed, organic matter accounts for about 20% of the total mass in comet Halley, more recently, the infrared features of organic compounds were detected in asteroids. The on-going Rosetta mission is being crucial to characterize this elusive material in a comet nucleus.

1 Introduction

This contribution is dedicated to the processes that occur in inter- and circumstellar ice, when dust grains accrete an ice mantle and molecules in the ice eventually desorb to the gas phase. Thermal desorption is of course very efficient at temperatures above the sublimation temperature of the various molecular ice components, namely H₂O, CO, CO₂, CH₃OH, NH₃, etc. Laboratory simulations can serve to improve our understanding of the accretion and

desorption processes in ice mantles. This work has direct implications for the formation of minor bodies in solar systems. The on-going measurements with Rosetta instrumentation of molecules desorbing from the nucleus of comet 67P/Churyumov-Gerasimenko can be better understood using laboratory data acquired during temperature programmed desorption experiments of cometary ice analogs containing a mixture of molecular species.

In the coldest regions, the short accretion time scales relative to the cloud lifetime, and the abundances of molecules in the gas observed toward dense cloud interiors, suggests that a non-thermal desorption mechanism like photo-desorption must be active in these environments. For this reason, in recent years much attention was paid to the study of photo-desorption processes experimentally. First, the photodesorption rates of several pure ices (CO, CO₂, H₂O, etc.) in the vacuum-ultraviolet range (VUV) was measured per incident photon. More recently, the measurements of VUV-absorption cross sections of molecular ices are allowing the estimation of the photodesorption rates per absorbed photon in the ice. These values can then be used as input in computational models to study the evolution of interstellar and circumstellar regions where ice mantles are present.

The experiments dedicated to ice processing suggest that the irradiation and warm-up of pre-cometary ice in circumstellar regions leads to the formation of organic matter of potential interest for prebiotic chemistry. In addition to VUV and X-ray photons, ions (cosmic rays) covering a broad energy spectrum are responsible for the energetic processing of ice in space. During the last five decades, numerous laboratory experiments were dedicated to study ice irradiation, in particular the destruction and the formation of new species during the irradiation, or later, after warm-up of the irradiated ice sample. Unfortunately, the detection of irradiation products in the ice is a difficult task: remote observations of solids in space rely mainly on infrared spectroscopy and simple molecules hinder the detection of other molecules with expected low abundances. Some of the relatively complex organic species that, according to laboratory simulations of ice irradiation and warm-up, could be present in ice mantles include carboxylic acids, alcohols, amides, amines, or amino acids. These species might be present in some comets like Halley, since these minor bodies contain ice and organic matter of a (yet) unknown composition. The ambitious Rosetta mission is, as we write these lines, making reality one of our dreams as molecular astrophysicists: to know what comets are made of and to what extent these primitive objects contributed to convert the early Earth into a living planet.

In this paper, we will first introduce the experiments dedicated to the simulation of ice processes in space environments, Sect. 2. The physical and chemical processes that occur in ice mantles are presented: the accretion and desorption is discussed in Sects. 3 and 4, ice irradiation is introduced in Sect. 5. Then, we will apply the experimental data on ice analogues to interpret some preliminary results obtained by the Rosetta mission, Sect. 6. The conclusions and future perspectives in the context of ice and organics in space are provided in Sect. 7.

2 Laboratory simulations of ice processes in space

Experimental simulations of ice mantle build-up on dust grains include the deposition of a gas mixture onto a cold substrate, containing some of the most abundant molecular components in ice mantles: H₂O, CH₃OH, CO, CO₂, CH₄, and NH₃. The ice is deposited at $T \approx 10$ K under vacuum conditions, with base pressures in the 10^{-7} – 10^{-11} mbar range. The physical and chemical evolution of the ice as the result of warm-up or irradiation is monitored *in situ* by FTIR spectroscopy. Other analytical tools are also useful to follow changes in the ice, including Raman and UV spectroscopy. The gas phase is commonly monitored during the experiment by quadrupole mass spectrometry (QMS).

The temperature programmed desorption (TPD) technique consists on the controlled warm-up of the ice using a heating ramp of typically 1 K min^{-1} . The ice is monitored by IR spectroscopy, allowing the detection of structural changes and the measurement of the decrease in ice thickness during the sublimation. Based on IR spectroscopy in transmittance, the ice column density is estimated by integration of the absorption bands, using the formula

$$N = \int_{\text{band}} \frac{\tau_\nu d\nu}{A} \quad (1)$$

where N is the column density in cm^{-2} , τ_ν the optical depth of the band, $d\nu$ the wavenumber differential in cm^{-1} , and A the band strength in cm molecule^{-1} . The integrated absorbance is equal to $0.43 \times \tau$, where τ is the integrated optical depth of the band. The QMS allows the detection of the desorbed ice molecules in the gas. The desorption rate, in molecules $\text{cm}^{-2} \text{ s}^{-1}$, of a given ice, for instance CO ice, is given by the Polanyi-Wigner equation

$$\frac{dN_{\text{g}}(\text{CO})}{dt} = \nu_i [N_{\text{s}}(\text{CO})]^i \exp\left(-\frac{E_{\text{d}}(\text{CO})}{T}\right) \quad (2)$$

where $N_{\text{g}}(\text{CO})$ is the column density of CO molecules desorbing from the ice surface (cm^{-2}), ν_i a frequency factor ($\text{molecules}^{1-i} \text{ cm}^{-2(1-i)} \text{ s}^{-1}$) for desorption order i , $N_{\text{s}}(\text{CO})$ the column density of CO molecules on the surface at time t , $E_{\text{d}}(\text{CO})$ the binding energy in K, and T the surface temperature in K. The TPD data can be fitted using this equation and the relation

$$\frac{dN_{\text{g}}(\text{CO})}{dt} = \frac{dT}{dt} \frac{dN}{dT} \quad (3)$$

where $\frac{dT}{dt}$ is the heating rate.

The experiments dealing with ice processing as the result of irradiation, mimicking photon and cosmic-ray processing of ice mantles in space, are summarized in Sect. 5.

3 Accretion and thermal desorption of ice

In this section, we selected the CO molecule, but the same expressions of the accretion and desorption hold for other molecules present in astrophysical ices, except for the case of photodesorption, which is presented in Sect. 4. The rates of accretion $R_{\text{acc}}(\text{CO})$, thermal

desorption $R_{\text{th-des}}(\text{CO})$, and photodesorption $R_{\text{ph-des}}(\text{CO})$ can be estimated as a function of time using the equations provided below. In the case of quiescent dark cloud interiors, where no processing by external UV flux occurs, the UV photon flux induced by cosmic rays is $F \sim 1 \times 10^4 \text{ photons cm}^{-2} \text{ s}^{-1}$. The initial cloud parameters are typically: $T_{\text{gas}} = T_{\text{dust}} \sim 10 \text{ K}$ are the gas and dust temperatures, $n_{\text{H}} = 1 - 3 \times 10^4 \text{ cm}^{-3}$ and $n_{\text{CO}} = 9.5 \times 10^{-5} \times n_{\text{H}}$ are the densities of H and CO. The masses of H and CO in grams are m_{H} and m_{CO} , and $m_{\text{CO}}(\text{amu}) = 28 \text{ amu}$ for CO. A dust density of $n_{\text{dust}} = \frac{0.01 \cdot n_{\text{H}} \cdot m_{\text{H}}}{1.33 \cdot \pi \cdot \rho \cdot r^3} = 1.33 \times 10^{-12} \cdot n_{\text{H}}$ dust grains is often assumed, with a constant radius $r = 0.05 \times 10^{-4} \text{ cm}$ and density $\rho = 3 \text{ g cm}^{-3}$ (silicate core density). The sticking probability near 10 K is expected to be close to unity, $f = 1$.

The rate of ice mantle build-up is

$$\frac{dn_{\text{s}}(\text{CO})}{dt} = R_{\text{acc}}(\text{CO}) - R_{\text{th-des}}(\text{CO}) - R_{\text{ph-des}}(\text{CO}). \quad (4)$$

The accretion rate of CO molecules onto grains is given by

$$R_{\text{acc}}(\text{CO}) = n_{\text{g}}(\text{CO}) \cdot n_{\text{dust}} \cdot \pi \cdot r^2 \cdot \sqrt{\frac{3 \cdot k \cdot T_{\text{gas}}}{m_{\text{CO}}}} \cdot f \quad (5)$$

in molecules $\text{cm}^{-3} \text{ s}^{-1}$, where k is the Boltzmann constant.

The thermal desorption of CO is

$$R_{\text{th-des}}(\text{CO}) = \nu_0(\text{CO}) \cdot \exp\left(-\frac{E_{\text{d}}(\text{CO})}{T_{\text{dust}}}\right) \cdot n_{\text{dust}} \cdot 4 \cdot \pi \cdot r^2 \quad (6)$$

in molecules $\text{cm}^{-3} \text{ s}^{-1}$, with $\nu_0(\text{CO}) = 6.5 \times 10^{26} \text{ molecules cm}^{-2} \text{ s}^{-1}$ and $E_{\text{d}}(\text{CO}) = 834 \text{ K}$, see Polanyi-Wigner equation in Sect. 2. In the next section we introduce the ice photodesorption.

4 Photo-desorption of ice

In the cold interiors of dark molecular clouds, most molecules are expected to stick to grains, thereby leading to depletion in the gas phase. CO was expected to deplete onto grains at temperatures below 20 K, but it is observed in the gas phase toward cold cloud interiors. In addition to photodesorption, the desorption induced by cosmic rays is expected to play an important role inside dense clouds.

At temperatures near 10 K, $R_{\text{th-des}}(\text{CO}) = 0$, and therefore $R_{\text{ph-des}}(\text{CO})$ drives the desorption. It was found experimentally for CO ice that the photodesorption rate decreases only when the ice thickness is less than about 5 monolayers (one monolayer, abbreviated as ML, corresponds to an ice thickness of one molecule, or a column density of $1 \times 10^{15} \text{ molecules cm}^{-2}$), which was interpreted as follows: a molecule on the ice surface can become excited and photodesorb after absorbing one photon, but molecules on the surface can also photodesorb if they receive the excess photon energy from another excited molecule, provided that there are no more than about three molecules between the photon excited molecule and the photodesorbed molecule. Therefore, based on laboratory results, for ice thicknesses

$x = \frac{n_s(\text{CO})(t)}{10^{15} \cdot n_{\text{dust}} \cdot 4 \cdot \pi \cdot r^2} < 5 \text{ ML}$, where $n_s(\text{CO})(t) = n_g(\text{CO})(0) - n_g(\text{CO})(t)$, the photodesorption rate can be expressed as

$$R_{\text{ph-des}}(x < 5\text{ML})(\text{CO}) = F \cdot (1 - e^{-\sigma N}) \cdot QY \cdot n_{\text{dust}} \cdot \pi \cdot r^2, \quad (7)$$

in molecules $\text{cm}^{-3} \text{ s}^{-1}$, and for $x \geq 5 \text{ ML}$ where $R_{\text{ph-des}}(\text{CO})$ is constant we have that

$$R_{\text{ph-des}}(x \geq 5\text{ML})(\text{CO}) = F \cdot (1 - e^{-\sigma 5 \times 10^{15}}) \cdot QY \cdot n_{\text{dust}} \cdot \pi \cdot r^2, \quad (8)$$

in molecules $\text{cm}^{-3} \text{ s}^{-1}$. Here F is the UV flux in photons $\text{cm}^{-2} \text{ s}^{-1}$, N is the ice column density, and QY is the quantum yield, i.e. the number of photodesorbed molecules per incident UV photon. For more details, we refer to the original publication [37].

There is a clear correspondence between the photodesorption rates measured for different monochromatic photon energies and the VUV absorption spectrum for the same photon energies. This indicates that photodesorption of some ice species like N_2 and CO is mainly driven by a desorption induced by electronic transition (DIET) process [16, 17]. The photodesorption rate of an ice, expressed in photodesorbed molecules per incident photon, will depend on the ice thickness. It is therefore more relevant to estimate the photodesorption rate as the number of photodesorbed molecules per absorbed photon.

The photodesorption rate per absorbed photon for the UV field present in interstellar regions, or the emission range of the UV lamp in simulation experiments, $R_{\text{ph-des}}^{\text{abs}}$, can be estimated as follows

$$R_{\text{ph-des}}^{\text{abs}} = \frac{I_0}{I_{\text{abs}}} R_{\text{ph-des}}^{\text{inc}} \quad (9)$$

where $R_{\text{ph-des}}^{\text{inc}}$ is the photodesorption rate per incident photon in the ice and

$$I_{\text{abs}} = \sum_{\lambda_i}^{\lambda_f} I_0(\lambda) - I(\lambda) = \sum_{\lambda_i}^{\lambda_f} I_0(\lambda)(1 - e^{-\sigma(\lambda)N})$$

and I_0 is the total photon flux emitted (in photons $\text{cm}^{-2} \text{ s}^{-1}$), I_{abs} is the total photon flux absorbed by the ice, $I_0(\lambda)$ is the photon flux emitted at wavelength λ , $\sigma(\lambda)$ is the VUV absorption cross section at the same wavelength, and N is the column density of the ice sample. Therefore, if the VUV absorption cross section of a given ice composition is known, it is possible to know what is the efficiency of the photodesorption per absorbed photon; in the case of N_2 and CO ices, for VUV photon energies that do not lead to direct dissociation of the molecules in the ice, we found that these values are higher than unity. For this reason, we recently estimated the VUV absorption cross sections of the common molecular ice components [13, 14, 15].

The values of $R_{\text{ph-des}}^{\text{abs}} > 1$ and the fact that the photons absorbed in ice monolayers deeper than the top monolayers (up to 5 for CO) can lead to a photodesorption event, indicate that the excess photon energy is transmitted to neighboring molecules in the ice within a certain range (we mentioned above that this range may correspond to about 5 monolayers in the case of CO ice; if a molecule on the ice surface receives sufficient energy from a molecule that received a photon, it may photodesorb [37]).

5 Ice irradiation and the formation of organic products

Laboratory analogs of interstellar ice submitted to irradiation, by photons (UV or X-rays) or ions (cosmic ray analogs) produce radicals and other fragments, which react during warm-up of the irradiated ice, forming new molecules [23]. After warm-up to room temperature, the organic refractory (o.r.) material formed, often called residue, contains complex organic compounds [1, 7, 4, 34, 5, 35, 32, 40, 9, 41, 28, 29].

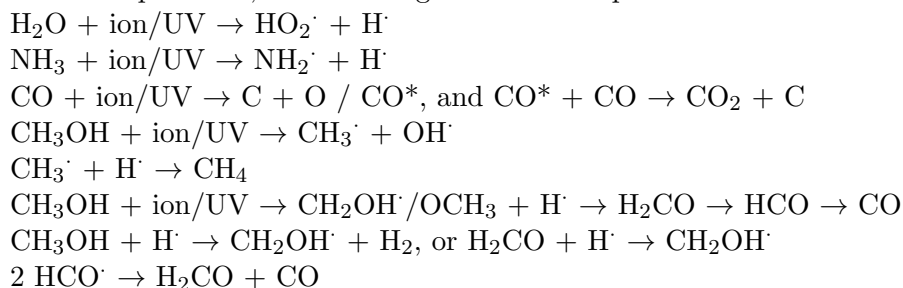
H₂O is generally the most abundant molecular component in interstellar and circumstellar icy grain mantles; it plays a key role as a starting ice component in irradiation and thermal processes leading to refractory products. The presence of substantial amounts of H₂O in the ice mixture leads to appreciable conversion of H₂CO to residue [44]. The formation of o.r. products is enhanced when the ice components are diluted in a H₂O ice matrix. An ice mixture containing H₂O:NH₃:CH₃OH = 20:1:1 led to the highest product formation, 28.4% of the carbon in the ice was converted to o.r. products, compared to 1.5% for the NH₃:CH₃OH = 1:1 mixture [35]. Another effect of H₂O photolysis is the formation of OH radicals that are incorporated into some of the products [35]. Therefore, the presence of OH groups in some of the o.r. species is related to H₂O photolysis or to CH₃OH induced reactions. The major effects of increasing the H₂O concentration in the ice mixture have been reported [42].

The main component of organic refractory is usually hexamethylenetetramine (HMT, [(CH₂)₆N₄]) if methanol is among the ice components. A small amount of HMT, about 1% of the o.r., is made from ice mixtures containing CO and no CH₃OH as the carbon source [7, 35]. The presence of ammonium salts of carboxylic acids [(R-COO⁻)(NH₄⁺)], amides [H₂NC(=O)-R] and esters [R-C(=O)-O-R'] [4, 35] is also inferred from their infrared fingerprints. Based on chromatographic analysis, carbamic acid, glycine, other amino acids or their precursors, and N-heterocyclic molecules are present with an abundance of the order of ~ 1% by number of molecules [34, 32, 40, 9, 28, 29]. Glycine and carbamic acid were detected before HCl-hydrolysis of o.r. [34, 9]. N-heterocycles in o.r., after hydrolysis, could act as precursors of the more complex amino acids detected (e.g. it is known that HCl-hydrolysis of the hydantoin imidazolidine-2,4-dione, one of the N-heterocycles present in o.r., leads to glycine formation) [34, 29]. In experiments dealing with circularly polarized UV irradiation of interstellar ice analogs, a small enantiomeric excess was measured [28]. If the concentration of H₂O in the starting ice mixture is low compared to the other ice components, species based on polyoxymethylene [(-CH₂O-)_n] are the most abundant.

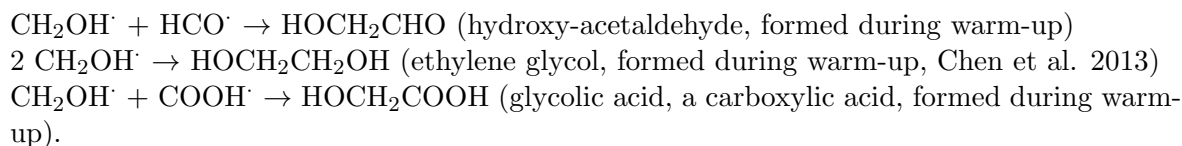
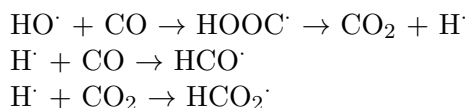
The reaction network induced by ion- or photo-processing of H₂O:CO:CH₃OH:NH₃ ice mixtures, followed by thermal processing, is highly complex. It appears that the formation of organic products due to photon or ion processing of various ice mixtures is quite similar, although some differences may be expected [38]. During irradiation, similar species are formed regardless of the radiation source. It is important that the warm-up process follows the same protocol in the UV and the ion experiments, because the reactions leading to the more complex species generally occur during heating of the irradiated ice, which allows radicals and ions to recombine and form new molecules. A reaction network for ice irradiation is provided below. The functional groups of the photoproducts were identified by IR spectroscopy, while some individual molecules were detected by chromatography coupled to mass spectrometry

([1] and ref. therein; ammonium salt and carboxylic acid formation was proposed [35]).

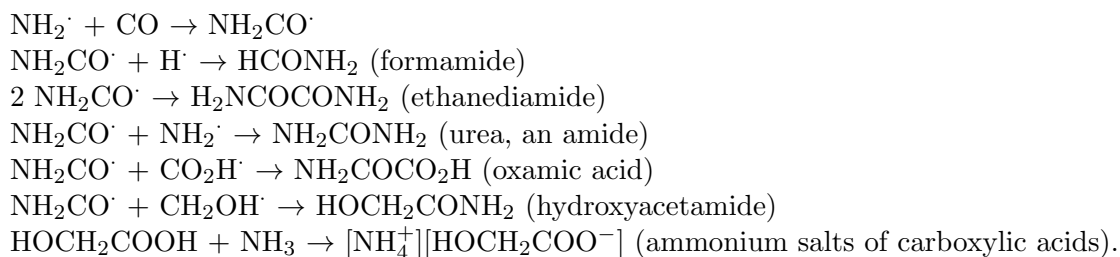
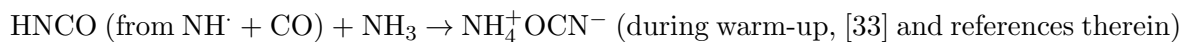
For pure ices, the following reactions are possible:



For ice mixtures:



The NH_x radicals allow the formation of a variety of new species; most of them are produced during the warm-up of the irradiated ice:



6 Some preliminary Rosetta results on cometary ice

Comets are expected to preserve the most pristine material in the solar system as their high abundances of volatiles indicate. These bodies are thought to be formed by agglomeration of dust particles of pre-solar and/or solar nebula origin in rather cold environments up to the outer parts of the solar nebula [22, 25]. However, the detection of crystalline silicates in

comets, as inferred from infrared observations [12], and the analysis of the dust collected by the Stardust mission during flyby of Comet Wild 2, indicate that not all comets are made of pristine material that was kept cold since its formation [8]. Indeed, the presence of high-temperature mineral grains suggests that at least some cometary grains were reprocessed in regions near the early Sun and ejected by radial mixing to the outer regions of the nebula [45, 6], where subsequently gas phase species would accrete onto such grains forming ice mantles.

Other parameters lead to a similar conclusion. The D/H ratio in water provides information about the origin of cometary materials. A D/H ratio around 3×10^{-4} was estimated for six comets considered to have originated in the Oort Cloud. This value is double the D/H ratio in water on Earth, i.e. 1.558×10^{-4} . It was thus concluded that at most 10% of oceanic water is of cometary origin [10]. But the first measurement of the D/H ratio in water from a Jupiter-family comet, 103P/Hartley 2, which originated in the Kuiper belt, gave a value of $(1.61 \pm 0.24) \times 10^{-4}$, very close to that of ocean water, which leaves open the possibility of a substantial contribution of water from Kuiper belt comets to oceanic water on Earth [24]. The isotopic ratios of many elements in comets, in particular the H and N fractionations, are consistent with temperatures near 50 K, compatible with the outer solar nebula regions [2]. Very recently, the high D/H ratio of water in Jupiter family comet 67P/Churyumov-Gerasimenko, $(5.3 \pm 0.7) \times 10^{-4}$, measured by the ROSINA mass spectrometer aboard Rosetta, a very high value [3]. Therefore, it is not possible to make a general statement on the origin of the different comet populations until more data has been gathered, for a sufficiently large number of comets.

The VIRTIS instrument of Rosetta measured a surface temperature 20 – 30 °C warmer than expected for a comet covered exclusively in ice, an indication of a dark material like dust. The images confirmed the detection of ubiquitous dust on the surface of the comet. The TPD experiments of ice mixtures with up to five molecular components predicted the detection of volatiles (CO, CO₂, NH₃, CH₃OH, etc.), including the more refractory H₂O, right after the arrival of Rosetta to the comet [30]. This prediction was confirmed: water was unexpectedly detected by the MIRO team. A few days later volatile species with lower abundances, of about 10% with respect to H₂O, were also observed. Basically, our prediction assumed a typical cometary albedo of 0.054, which means that the temperature on the comet surface should be near 141 K at a distance of 3.8 AU from the Sun. The estimated heating rate of the comet is about 3 K per month. Therefore, we expected that the desorption of water on the comet surface would occur below 130 K, which was lower than the surface temperature estimated during arrival, 141 K.

As predicted by J. Oró [43], cometary dust is rich in carbonaceous/organic matter, as much as 50% by mass for Comet Halley, although this proportion varies among comets [19]. A large fraction of the carbon matter in Halley, about 50%, is oxygen-rich (i.e. this matter has O/C \geq 0.5); these compounds are consistent with structures of alcohols, aldehydes, ketones, acids and amino acids, and their salts. The exact make-up of these molecules could not be unambiguously identified [18, 19]. Low O and H and high N contents were reported for Comet Wild 2 [27]. While laboratory analysis of the inorganic composition in Stardust samples served to identify several minerals, contamination and annealing of the

carbon fraction during capture on the aerogel collector made the characterization of the carbon fraction a difficult task [36].

The Rosetta mission attempts to analyze *in situ* the composition of a comet nucleus. The detection of organic species such as amino acids in the cometary nucleus is the main goal of the COSAC mass spectrometer [20, 21]. The non-nominal landing of Philae, the lander of Rosetta, was likely responsible for the poor signals measured after drilling the comet surface. Only one measurement could be performed by the COSAC gas chromatograph-mass spectrometer. If enough battery power is accumulated in the coming months, this measurement could be repeated. Luckily, the COSAC and Ptolemy instruments in the sniffing mode (only mass spectrometry) detected a number of molecules near the surface during the landing sequence. These species are currently being identified, but they are similar to the photoproducts made by ice irradiation and warm-up in the laboratory, see Sect. 5.

7 Conclusions and future prospectives

We introduced the laboratory experiments dedicated to simulate ice processes in various astrophysical environments. The fundamentals of accretion, thermal desorption and photodesorption were also presented. These processes are essential to understand the formation of ice mantles and the observations of molecules in the gas toward cold interstellar and circumstellar regions. We applied the temperature programmed desorption of ice mixtures to predict the detection of cometary volatiles as a function of surface temperature in comet Churyumov-Gerasimenko, the main target of the ESA-Rosetta mission. It was, therefore, not a surprise for our team that water molecules ejected from the comet nucleus were detected right after the arrival of the Rosetta orbiter to this comet and, naturally, more volatile species like CO and CO₂ would have desorbed prior to water.

Experiments show that photoprocessing of ice mantles, which likely took place in the local dense cloud and/or the solar nebula, leads to a variety of molecules of biochemical relevance. Some of these molecules may be stored in comets and minor bodies of solar systems.

There are significant similarities between the organics found in comets and meteorites and the organic refractory residues produced by ice photoprocessing in the laboratory. Glycolic acid, the most abundant carboxylic acid produced by ice UV-photoprocessing and warmup [1, 7], was found in the Murchison meteorite [11]. The N-heterocycles present in organic residues are similar to those inferred from the data of comet Halley [26]. Amino acids and diamino acids and/or their precursors also result from ice photoprocessing and warm-up [34, 5]. Most of these amino acids are common to the Murchison meteorite. Based on the detection of diamino acids in the organic residues, the presence of diamino acids in Murchison was first predicted [34] and they were later detected [31]. Amino acids are the components of proteins and diamino acids are peptide nucleic acid (PNA) components, a possible precursor of RNA. This suggests that energetic processing of ice in the local dense cloud and the solar nebula could be significant. Strecker synthesis could explain the formation of species like α -amino acids on meteorite parent bodies where aqueous alteration took place, but does not

explain the presence of organics in comets where water is in the solid state. It was proposed that the organic globules observed in some meteorites, with elevated D/H and $^{15}\text{N}/^{14}\text{N}$ ratios indicative of low temperature formation, are the result of ice mantle UV-irradiation [39].

Cometary impacts were likely the most favorable way to deliver prebiotic species to the primitive Earth. Unfortunately, the organic analysis of cometary Stardust samples faced problems with contamination. The new data provided by Rosetta instruments on the comet morphology and composition is very precious. In the coming months, the identification of organic molecules in a cometary nucleus will be published, and there remains the possibility of making new measurements during 2015, once the batteries of Philae are reloaded.

Acknowledgments

This work has been supported by the Spanish MICINN/MINECO under projects AYA2011-29375 and CONSOLIDER grant CSD2009-00038.

References

- [1] Agarwal, V. K., Schutte, W. A., Greenberg, J. M., et al. 1985, *Origins Life Evol. Biospheres*, 16, 21
- [2] Aleon, J., & Robert, F. 2004, *Icarus*, 167, 424
- [3] Altwegg, K., Balsiger, H., Bar-Nun, A., et al. 2015, *Science*, 347, A1261952
- [4] Bernstein, M. P., Sandford, S. A., Allamandola, L. J., Chang, S., & Scharberg, M. A. 1995, *ApJ*, 454, 327
- [5] Bernstein, M. P., Dworkin, J. P., Sandford, S. A., Cooper, G. W., & Allamandola, L. J. 2002, *Nature*, 416, 401
- [6] Bockelée-Morvan, D., Gautier, D. Hersant, F., Huré, J.-M., & Robert, F. 2002, *A&A*, 384, 1107
- [7] Briggs, R., Ertem, G., Ferris, J. P., et al. 1992, *Origins Life Evol. Biospheres*, 22, 287
- [8] Brownlee, D. E., & Stardust Team, AAS DPS Meeting #38, 2006, abs. #23.02
- [9] Chen, Y.-J., Nuevo, M., Hsieh, J.-M. et al. 2007, *A&A*, 464, 253
- [10] Cottin, H. Szopa, C., & Moore, M. H. 2001, *ApJ*, 561, L139
- [11] Cronin, J. R., Pizzarello, S., & Cruikshank, D. P., in *Meteorites and the Early Solar System 1988*, eds. J. F. Kerridge and M. S. Matthews (Tucson: Univ. of Arizona Press), 819
- [12] Crovisier, J., Leech, K., Bockelée-Morvan, D. et al. 1997, *Science*, 275, 1904
- [13] Cruz-Diaz, G. A., Muñoz Caro, G. M., Chen, Y.-J., & Yih, T.-S. 2014, *A&A*, 562, A120
- [14] Cruz-Diaz, G. A., Muñoz Caro, G. M., Chen, Y.-J., & Yih, T.-S. 2014, *A&A*, 562, A119
- [15] Cruz-Diaz, G. A., Muñoz Caro, G. M., & Chen, Y.-J. 2014, *MNRAS*, 439, 2370
- [16] Fayolle, E. C., Bertin, M., Romanzin, C., Michaut, X., Oberg, K. I., et al. 2011, *ApJ Letters*, 739, L36

- [17] Fayolle, E. C., Bertin, M., Romanzin, C., Poderoso, H. A. M., Philippe, L., et al. 2013, *A&A*, 556, A122
- [18] Fomenkova, M. N., Chang, S., & Mukhin, L. M. 1994, *Geochim. Cosmochim. Acta*, 58(20), 4503
- [19] Fomenkova, M. N. 1999, *Space Sci. Rev.*, 90, 109
- [20] Goesmann, F., Rosenbauer, H., Roll, R. et al. 2007, *Space Science Reviews*, 128, 257
- [21] Goesmann, F., Raulin, F., Bredehöft, J. H., et al. 2014, *P&SS*, 103, 318
- [22] Greenberg, J. M., in *Comets 1982*, ed. L. L. Wilkening (Tucson: Univ. Arizona Press), 131
- [23] Hagen, W., Allamandola, L. J., & Greenberg, J. M. 1979, *Ap&SS*, 65, 215
- [24] Hartogh, P. Lis, D. C., Bockelée-Morvan, D., et al. 2011, *Nature*, 478, 218
- [25] Irvine, W. M., Schloerb, F. P., Crovisier, J., Fegley, B. Jr., & Mumma, M. J., in *Protostars and Planets IV*, 2000, eds. V. Mannings, A. P. Boss and S. S. Russell (Tucson: Univ. Arizona Press), 1159
- [26] Kissel, J., & Krueger, F. R. 1987, *Nature*, 326, 755
- [27] Kissel, J., Krueger, F. R., Silén, J., & Clark, B. C. 2004, *Science*, 304, 1774
- [28] de Marcellus, P., Meinert, C., Nuevo, M., et al. 2011, *ApJ*, 727, L27
- [29] de Marcellus, P., Bertrand, M., Nuevo, M., Westall, F., & d'Hendecourt, L. 2011, *Astrobiology*, 11, 847
- [30] Martín-Doménech, R., Muñoz Caro, G. M., Bueno, J., & Goesmann, F. 2014, *A&A*, 564, A8
- [31] Meierhenrich, U. J., Muñoz Caro, G. M., Bredehöft, J. H., Jessberger, E. K., & Thiemann, W. H.-P. 2004, *PNAS*, 101(25), 9182
- [32] Meierhenrich, U. J., Muñoz Caro, G. M., Schutte, W. A., Thiemann, W. H.-P., et al. 2005, *Chem.-Eur. J.*, 11, 4895
- [33] Mispelaer, F., Theule, P., Duvernay, F., Roubin, P., & Chiavassa, T. 2012, *A&A*, 540, A40
- [34] Muñoz Caro, G. M., Meierhenrich, U. J., Schutte, W. A., et al. 2002, *Nature*, 416, 403
- [35] Muñoz Caro, G. M., & Schutte, W. A. 2003, *A&A*, 412, 121
- [36] Muñoz Caro, G. M., Dartois, E., & Nakamura-Messenger, K. 2008, *A&A*, 485, 743
- [37] Muñoz Caro, G. M., Jiménez-Escobar, A., Martín-Gago, J. Á., et al. 2010, *A&A*, 522, A108
- [38] Muñoz Caro, G. M., Dartois, E., Boduch, P., et al. 2014, *A&A*, 566, A93
- [39] Nakamura-Messenger, K., Messenger, S., Keller, L. P., Clemett, S. J., & Zolensky, M. E. 2006, *Science*, 314, 1439
- [40] Nuevo, M., Meierhenrich, U. J., Muñoz Caro, G. M., et al. 2006, *A&A*, 2006, 457, 741
- [41] Nuevo, M., Milam, S. N., Sandford, S. A., et al. 2011, *Adv. Space Res.*, 48, 1126
- [42] Öberg, K. I., van Dishoeck, E. F., Linnartz, H., & Anderson, S. 2010, *ApJ*, 718, 832
- [43] Oró, J. 1961, *Nature*, 190, 389
- [44] Schutte, W. A., Allamandola, L. J., & Sandford, S. A. 1993, *Icarus*, 104, 118
- [45] Shu, F. H., Shang, H., Gounelle, M., Glassgold, A. E., & Lee, T. 2001, *ApJ*, 548, 1029